International Journal of Modern Physics E

COLLECTIVE MOTION IN NUCLEAR COLLISIONS AND SUPERNOVA EXPLOSIONS

WOLFGANG BAUER
Department of Physics and Astronomy, Michigan State University, and National Superconducting Cyclotron Laboratory, East Lansing, MI 48824, USA
bauer@pa.msu.edu

TERRANCE STROTHER
Department of Physics and Astronomy, Michigan State University, and National Superconducting Cyclotron Laboratory, East Lansing, MI 48824, USA
strother@nscl.msu.edu

Received (received date)
Revised (revised date)

Motivated by the success of kinetic theory in the description of observables in intermediate and high energy heavy ion collisions, we apply kinetic theory to the physics of supernova explosions. The algorithmic implementation for the high-density phase of the iron core collapse is discussed.

1. Introduction

Supernova explosions are believed to be one of the main sources for heavy element production ($A > 56$) in the universe. The exact mechanism for the origin of the heavy elements is one of the top eleven science questions for the new century in the report *Connecting Quarks with the Cosmos*[1]. The answer to this question is sought in two complementary ways, through construction and operation of rare isotope acceleration facilities, and through astronomical observation of supernova explosions and their computer modeling. It is this latter subject to which the present article attempts to contribute.

The simulation of supernova explosions on the computer[2,3,4,5,6,7,8] is still a task that strains and even exceeds the capabilities of the highest performance supercomputers. Typical numerical implementations rely on hydrodynamics codes for the baryons, coupled to a Boltzmann transport simulation for the neutrinos and other leptons. These simulations need to be implemented on grids in three dimensional coordinate systems, taking care of special relativity, causality, high density nuclear matter ($\rho_{\rm baryon} > 3\rho_0$), particle production, and huge magnetic fields that are generated self-consistently. Furthermore, the grids need to be fine-grained enough to allow the calculation of shock waves and turbulence. All of this needs to be accom-

plished in a system that rapidly contracts and then expands, and that needs to be followed over many thousands of time steps.

Nuclear collisions at intermediate and high energies provide similar challenges. Particle production also dominates the late stages of the collisions, and shock wave formation, collective deflection, as well as the interplay between regular and chaotic collective dynamics[9] can be observed. This collective motion includes transverse flow, radial flow, and elliptic flow. Transport theories based on semiclassical implementation of kinetic theory[10,11,12,13,14,15,16] have been incredibly successful in reproducing experimental observables and pointing the way to new physical insight into these systems. So it is tempting to implement these types of kinetic theory based approaches for the physics and astrophysics of supernova explosions. This is the aim of our work.

2. Basic Equations to be Solved

The one-body transport equation for the baryon phase space density $f_b(xk)$ is given by[17]

$$\frac{\partial f_b(xp)}{\partial t} + \frac{\Pi^i}{E_b^*(p)}\nabla_i^x f_b(xp) - \frac{\Pi^\mu}{E_b^*(p)}\nabla_i^x U_\mu(x)\nabla_p^i f_b(xp) + \frac{M_b^*}{E_b^*(p)}\nabla_i^x U_s \nabla_p^i f_b(xp) = I_{bb}^b(xp) + I_{b\nu}^b(xp) \tag{1}$$

for the particular state b of the baryon. For any neutrino species we have a simpler equation of motion that only contains the streaming term and the collision term, but no mean field contributions,

$$\frac{\partial f_\nu(xk)}{\partial t} + \frac{k\cdot\ \nabla^x}{E_\nu(k)} f_\nu(xk) = I_{b\nu}^\nu(xk)\ . \tag{2}$$

The baryon-baryon collision term, I_{bb}^b, is given by

$$I_{bb}^b(xp) = \frac{\pi}{(2\pi)^9}\sum_{\alpha_1\alpha_2\alpha_3, m_s^b}\int\int\int dp_1 dp_2 dp_3 \frac{M_b^* M_{\alpha_1}^* M_{\alpha_2}^* M_{\alpha_3}^*}{E_b^* E_{\alpha_1}^* E_{\alpha_2}^* E_{\alpha_3}^*} \tag{3}$$
$$\delta(E_b^*(p) + E_{\alpha_1}^*(p_1) - E_{\alpha_2}^*(p_2) - E_{\alpha_3}^*(p_3))\delta(\ p + \ p_1 - \ p_2 - \ p_3)\langle\langle\mathcal{M}_{bb}\rangle\rangle$$
$$[f_{\alpha_2}(xp_2) f_{\alpha_3}(xp_3)\overline{f}_{\alpha_1}(xp_1)\overline{f}_b(xp) - \overline{f}_{\alpha_2}(xp_2)\overline{f}_{\alpha_3}(xp_3) f_{\alpha_1}(xp_1) f_b(xp)]\ .$$

We use the notation $\overline{f}_b(xk) \equiv 1 - f_b(xk)$. The factors $\overline{f}_b(xk)$ are a consequence of the Pauli Exclusion Principle for the final scattering states. The matrix elements $\langle\langle\mathcal{M}_{bb}\rangle\rangle$ do not need to be evaluated explicitly, because we operate in the hydrodynamic limit. Similar collision terms can be derived for the neutrino-baryon collisions[17], in analogy to our earlier work on coupled transport equations for heavy ion collisions[18].

In order to solve the above transport equations, we utilize the test particle method,[19] where we represent the phase space distribution function by a sum over delta functions,

$$f(xp) = \Sigma_i \delta(x - x_i)\delta(p - p_i)\ . \tag{4}$$

The initial coordinates of these delta-function point particles (= test particles) have to be determined by some physical input model. For nuclear collisions a local Thomas-Fermi approximation, properly Lorentz-boosted, is sufficient. For our supernova progenitor, we use initial conditions provided by the rotating core model.[20]

With this approach we can derive first order differential equations for the centroid coordinates of these test particles as

$$\frac{d}{dt}p_j = -\nabla U_{EoS,e^-}(r_j) + F_{G,j} + \mathcal{C}(p_j) + \mathcal{C}_\nu(p_j) \tag{5}$$

$$\frac{d}{dt}r_j = \frac{p_j}{\sqrt{m^2 + p_j^2}} \tag{6}$$

$$j = 1, \ldots, N \ , \tag{7}$$

where $\mathcal{C}(p_j)$ and $\mathcal{C}_\nu(p_j)$ symbolize the effects of two-body collisions with other baryons and neutrinos, respectively, on the test particle momenta. N is the number of test particles used and should be at least 10^6, but 10^8 or even larger is also technically feasible with present-day computers.

3. Numerical Implementation

Since we are forced to work with a very large number of test particles, we need to avoid processes and algorithms that scale with N^2 or even N^3. This is not easy, because two-body collisions usually involve double loops over all particles. If the final state occupancies are important, then even triple loops come into play. In order to circumvent these difficulties, we employ a modified Direct Simulation Monte Carlo technique for the two-body collision processes. This type of algorithm was previously used by us in the simulation of heavy ion collisions as well.[21]

In the latest version of our code, the test particle based simulations of a collapsing stellar core are run inside two static Cartesian grids. The location of the test particles in both of these grids is known at all times along with their Cartesian coordinates and momenta. The motion of the test particles in the grids is tracked by computing the momentum of each test particle as well as the force acting on it, in each iteration of the code, and using a forth order Rung-Kutta method to solve for the new position and momentum. The two grids are cubic and independent of each other. One of the grids is used to determine the mass density at arbitrary points and is called the density grid while the other is used to allow test particles in each cell in the grid to collide with one another and is referred to as the collision grid. The grids are the same size, just large enough to inscribe the initially circular core, but they have a different number of cells. First let us focus our attention on the collision grid and its main purpose.

3.1. *Collision Grid and Two-Body Collisions*

This grids purpose is to allow test particles in the same cell to collide with one another. However, one must have a clever way of accessing test particles that are

located in a given cell. We address this issue by introducing a number called the collision index, I_c,

$$I_c = M^2 i_x + M i_y + i_z \tag{8}$$

where i_x, i_y, and i_z are the three cartesian coordinates of the cell, and $0 \leq i_x, i_y, i_z < M$. Employing a quicksort algorithm after each time step ensures that particles with the same value of I_c are stored next to each other in a one-dimensional array. In this way collision partners can be found in a very efficient way, with an algorithm that scales as $N \log N$. We believe that this is the fastest implementation of two-body collisions.

3.2. *Gravitational Force and Nuclear Force*

To calculate the exact Newtonian gravitational force on each test particle, we would again have to execute a double loop. The Newtonian monopole approximation looked like an appealing alternative, as it only required that the test particles be sorted by their radial distances from the origin each time the gravitational force was to be computed for all of the test particles. In this approximation, their radial rankings and distances were the only variables needed to determine the gravitational force acting on them.

$$F_{G,j} = -r_j \frac{G m^2 \#\{i \in \{1, \ldots, N\} : r_i < r_j\}}{r_i^3} \tag{9}$$

With an efficient quicksort-type algorithm, the CPU time requirements for the self-consistent calculation of gravity only scales as $N \log N$.

We found, however, that the Newtonian monopole approximation yielded unphysical results when applied to test particles near the origin. To avoid this complication, for the purpose of calculating the gravitational force, we assume the density is constant at all points within one tenth of the cores radius of the origin. This assumption is justified because in all previous simulations, the cores density distribution remained spherically symmetric in this region and always changed relatively little compared to the steep drop off in densities seen at larger radii. Therefore to approximate the gravitational force on all of the test particles, we use the Newtonian monopole approximation for all test particles whose radial coordinates are greater than one tenth of the cores radius R and a linear restoring force proportional to the magnitude of the force given by the Newtonian monopole approximation evaluated at one tenth of the cores radius for all test particles whose radial coordinates are less than or equal to one tenth of the cores radius. For all locations inside $R/10$, we interpolate linearly to 0, the value of the force at $r = 0$:

$$F_{G,j}(r < R/10) = F_{G,j}(R/10) \frac{r}{R} \tag{10}$$

In addition to the gravitational force, our simulations also have to include the nuclear force. In particular, it is very important to use an isospin dependent nuclear

equation of state, because the electron fraction changes quite strongly during the course of the collapse and explosion phases. In fact, this isospin dependent nuclear EoS provides a major area of common intellectual interest between astrophysics and nuclear physics[22]. Further numerical details on the one-body part of our simulations can be found in our earlier publications[23,24].

3.3. *Mass Density and Spatial Gradients*

In order to eliminate the dependence on particular implementations of a spatial grid, we introduce finite Gaussian density distributions for the test particles.

$$\rho(r, r_0) = k \exp[-(r - r_0)^2/2\sigma^2] \tag{11}$$

This method is similar to the so-called "smearing" algorithm employes in simulations of heavy ion collisions. A cutoff, $|r - r_0| < a$ ensures that our algorithm that follows from this procedure does not scale as N^2 due to an infinite-ranged Gaussian. The normalization constant k is of course a function of this cutoff length a.

Since we approximate the nuclear mean field potential by a density dependent functional, and since the mass density due to the test particles is now a sum of truncated Gaussians, we are able to provide exact expressions for the spatial gradients of the nuclear mean field force terms. This approach is then similar to the so-called "quantum molecular dynamics" algorithms that are utilized in nuclear physics.[25,26]

The main advantage of this method is that the grid size does not enter as a parameter any more. Thus one can achieve a much better spatial resolution, which is only limited by statistical fluctuations due to the finite number of test particles. This feature is extremely important if one wants to address the spatial localization of shock waves.

4. Role of Angular Momentum

If a rotating star collapses, conservation of angular momentum dictates that its angular frequency increases inversely proportional to the reduction of the moment of inertia. We hypothesize that this leads to the formation of rotation vortices along the axis of rotation. The baryon density at the "poles" will be reduced relative to the equatorial plane. Neutrinos can then escape much easier along the axis than perpendicular to it.

Our first studies of rotating collapsing iron cores bear out the hypothesis of formation of rotation vortices.

Figure 1 shows a preliminary result of a simulation of a rotating collapsing iron core of one solar mass. The rotation axis is defined as the z-axis of our coordinate system. One can clearly see that for radii larger than 150 km the baryon density in the equatorial plane greatly exceeds that along the poles.

We speculate that this formation of rotation vortices will be much enhanced once we have implemented a fully consistent treatment of the neutrino emission and propagation. This focussing of neutrino emission along the poles will amplify the

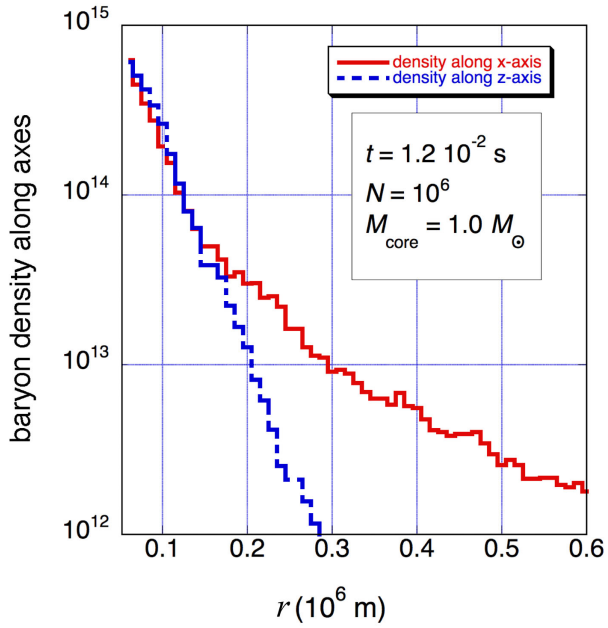

Fig. 1. Density along and perpendicular to the rotation axis, the z-axis, for a rotating collapsing iron core of one solar mass.

parity violation induced recoil kick scenario proposed for the neutron star remnant by Horowitz et al.[27,28] However, before we can reach quantitative conclusions to substantiate this claim, we will have to implement the aforementioned physics.

5. Summary

This simulation is not yet complete. The effects on neutrino production and scattering as well as magnetism have yet to built into the code. A self-consistent way of determining the electron fraction in three dimensions must also be implemented eventually.

However, our approach is able to provide a full three-dimensional description of the time evolution for baryons and eventually for neutrinos. The solution of this coupled problem requires only a factor of two to four more CPU time, as compared to the solution of the baryon dynamics alone. We realize that there are details regarding the widely varying interaction time scales that need to be worked out, and that might result in a bigger rise in CPU time than estimated here. But from our experience with perturbative sub-threshold particle production we are optimistic that these issue will be able to be worked out.

Effects of collective rotation can be modeled, as indicated by us here and shown in much more detail elsewhere.[23] Once all of the processes above are implemented, we will be able to compare with the results obtained by using the smooth-particle

hydrodynamics approach, where the influence of rotation was already examined.[29]

The new techniques introduced here that gives analytic expressions for the mass density at arbitrary points in the density grid has many advantages. It allow us to zoom in on any region of interest of the core when we generate images without any loss of resolution. Further, it allows use of the exact derivatives utilized in the calculation of the nuclear force on the test particles. Arguably the most important advantage to knowing the density at arbitrary points in the grid is the ability to see the exact propagation of density shockwaves. In the current implementation of our algorithm the grid size does not provide a lower limit for the spatial resolution. Instead, the spatial resolution scales as $N^{-1/2}$, where N is the number of test particles. This fact gives hope to large improvements in numerical accuracy once we are able to port our algorithms to massively parallel computer clusters.

Acknowledgment(s)

This research was supported by the US National Science Foundation under grant PHY-0245009 and an Alexander-von-Humboldt Foundation Distinguished Senior U.S. Scientist Award.

References

1. Committee on the Physics of the Universe, National Research Council, *Connecting Quarks with the Cosmos: Eleven Science Questions for the New Century* (National Academy Press, 2003).
2. J.R. Wilson, *Numerical Astrophysics* (Jones and Bartlett, Boston, 1985).
3. M. Herant, W. Benz, W.R. Hix, C.L. Fryer, and S.A. Colgate, Astrophys. J. **435** 339 (1994).
4. C.L. Fryer and A. Heger, *Astrophys. J.* **541** 1033 (2000).
5. R. Buras, M. Rampp, H.-Th. Janka, and K. Kifonidis, *Phys. Rev. Lett.* **90** 241101 (2003).
6. H.-Th. Janka, R. Buras, and M. Rampp, *Nucl. Phys. A* **718** 269c (2003).
7. A. Mezzacappa, M. Liebendörfer, O.E.B. Messer, W.R. Hix, F.-K. Thielemann, and S.W. Bruenn, *Phys. Rev. Lett.* **86** 1935 (2001).
8. T.A. Thompson, A. Burrows, and P.A. Pinto, *Astrophys. J.* **592** 434 (2003).
9. W. Bauer, D. McGrew, V. Zelevinsky, and P. Schuck, *Phys. Rev. Lett.* **72**, 3771 (1994).
10. G.F. Bertsch et al., *Phys. Rev. C* **29** 673 (1984).
11. H. Kruse et al., *Phys. Rev. Lett.* **54** 289 (1985).
12. W. Bauer, G.F. Bertsch, W. Gassing, and U. Mosel, *Phys. Rev. C* **34** 2127 (1986).
13. H. Stöcker, and W. Greiner, *Phys. Rep.* **137** 277 (1986).
14. G.F. Bertsch and S. Das Gupta, *Phys. Rep.* **160** 189 (1988).
15. P. Schuck et al., *Prog. Part. Nucl. Phys.* **22** 181 (1989).
16. W.G. Gong, W. Bauer, C.K. Gelbke, and S. Pratt, *Phys. Rev. C* **43** 781 (1991).
17. W. Bauer, submitted to *Heavy Ion Physics* (2004).
18. S.J. Wang, B.-A. Li, W. Bauer, and J. Randrup, *Annals of Physics* **209** 251 (1991).
19. C.-Y. Wong, *Phys. Rev. C* **25** 1460 (1982).
20. A. Heger, N. Langer, and S.E. Woosley, *Astrophys. J.* **528** 368 (2000).
21. G. Kortemeyer, F. Daffin, and W. Bauer, *Phys. Lett.* **B374**, 25 (1996).
22. B.-A. Li, C.M. Ko, and W. Bauer, Int. J. Mod. Phys. E **7**(2), 147 (1998).

23. T. Bollenbach and W. Bauer, in *Exotic Clustering*, edited by S. Costa, A. Insolia, and C. Tùve, American Institute of Physics Conference Proceedings, Volume **644** (Melville, New York, 2002) 219.
24. W. Bauer, Acta Phys. Hung. A **21**, 371 (2004).
25. J. Aichelin and H. Stöcker, *Phys. Lett.* **B176** 14 (1986).
26. H. Sorge, H. Stöcker, and W. Greiner, *Nucl. Phys.* **A498** 567C (1989).
27. C.J. Horowitz and Gang Li, *Phys. Rev. Lett.* **80** 3694 (1998).
28. C.J. Horowitz and J. Piekarewicz, *Nucl. Phys. A* **640** 281 (1998).
29. C.L. Fryer and M.S. Warren, Astrophys. J. **574** (2002), L65.